Scanning pentaprism test for the GMT 8.4 m off-axis segments

Richard Allen[a], Peng Su[b], James H. Burge[a,b], Brian Cuerden[a], Hubert M. Martin[a]

[a]Dept.of Astronomy/Steward Observatory, the Univ. of Arizona, Tucson, AZ 85721, U.S.A
[b]College of Optical Sciences, the University of Arizona, Tucson, AZ 85721,U.S.A.

ABSTRACT

The scanning pentaprism system for testing the 8.4 m off-axis segments for the Giant Magellan Telescope has recently been completed. The system uses a fiber source and a carriage mounted pentaprism to scan a 40 mm collimated beam across the surface of the segment under test. Since the scanning beam is parallel to the optical axis of the parent mirror, it comes to focus on a detector at the telescope's prime focus, where displacement of the spot is proportional to the slope error. A second collimated beam from a stationary reference pentaprism is used to compensate for any changes in the relative positions of the optical components during testing. The optical components are suspended over the mirror on a rail system that can be rotated so that scans can be made across any diameter of the segment. The test is capable of measuring wavefront slope errors to 1 μrad rms, adequate to verify that power, astigmatism, coma, and other low-order aberrations are small enough to be corrected easily at the telescope with the segment's active support system.

Keywords: Aspherics, telescope, optical testing

1. INTRODUCTION

The University of Arizona has developed several tests to guide the fabrication of the off-axis mirror segments for the Giant Magellan Telescope (GMT).[1]-[3] The Laser Tracker Plus system uses a high precision laser tracker to measure the position of a tracker ball that is scanned across the surface of the mirror. The principal optical test uses a hologram and two spherical mirrors to produce a wavefront that can be used to do an interferometric null test on the mirror. We have now implemented a scanning pentaprism test as an independent verification of the principal test.

Figure 1 illustrates the concept of the pentaprism test.[4],[5] A pentaprism test of a paraboloidal or near paraboloidal surface utilizes the property that incoming rays parallel to the optical axis will go through or near the focal point. The pentaprism system scans a narrow collimated beam across the surface, and a detector at the focus is used to measure the position of the focused spot. The displacement of the spot is proportional to slope errors on the mirror surface. A second pentaprism at a fixed location produces a reference spot that can be used to compensate for changes in system alignment as the mirror is scanned. Four scans along the paths shown in Figure 1 can be used to measure wavefront slope errors to an accuracy of 1 μrad rms and low-order polynomial terms to an accuracy on the order of 100 nm rms surface on an 8.4 m mirror. To obtain this accuracy with an off-axis mirror, it is necessary to carefully account for field aberrations that result when the collimated beam is not exactly parallel to the optical axis. These effects have been analyzed in previous papers[6],[7], and the results have been used in testing the 1.7 m off-axis primary mirror of the New Solar Telescope (NST). In this paper, we summarize the principles of the pentaprism test, including the field effects that are important for off-axis mirrors. We then summarize the NST measurements and describe the system that has recently been constructed for testing the first off-axis segment for the GMT.

The collimated source for the NST and GMT pentaprism tests consists of a single-mode fiber and a lens that is well-corrected for spherical aberration. The source is fed with 635 nm light from a laser diode. The fiber and lens are aligned so that the collimated output beam lies in a plane that is perpendicular to the parent axis shown in Figure 1. The output beam initially strikes a stationary reference pentaprism that has a built-in beamsplitter. Half of the incoming light is deflected 90° down toward the mirror. The other half travels to a pentaprism that can be positioned at different distances from the source. This pentaprism also deflects the incoming light by 90°. Since the output beams from both pentaprisms approach the mirror on paths that are parallel to the parent axis, the rays in both beams appear to come from a single on-axis source at infinity. In the case of a paraboloid such as the NST primary, both beams converge to a single spot on the camera at the focus of the parent mirror. Since the GMT primary is an ellipsoid with k = -0. 998286, the spots from the reference and the scanning prisms can be separated by as much as 900 μm, or 50 μrad of wavefront slope, even if the test system is perfectly aligned. In either case, slopes on the mirror are found by comparing the observed positions of the spots to the expected positions.

Modern Technologies in Space- and Ground-based Telescopes and Instrumentation, edited by Eli Atad-Ettedgui, Dietrich Lemke, Proc. of SPIE Vol. 7739, 773911 · © 2010 SPIE · CCC code: 0277-786X/10/$18 · doi: 10.1117/12.857901

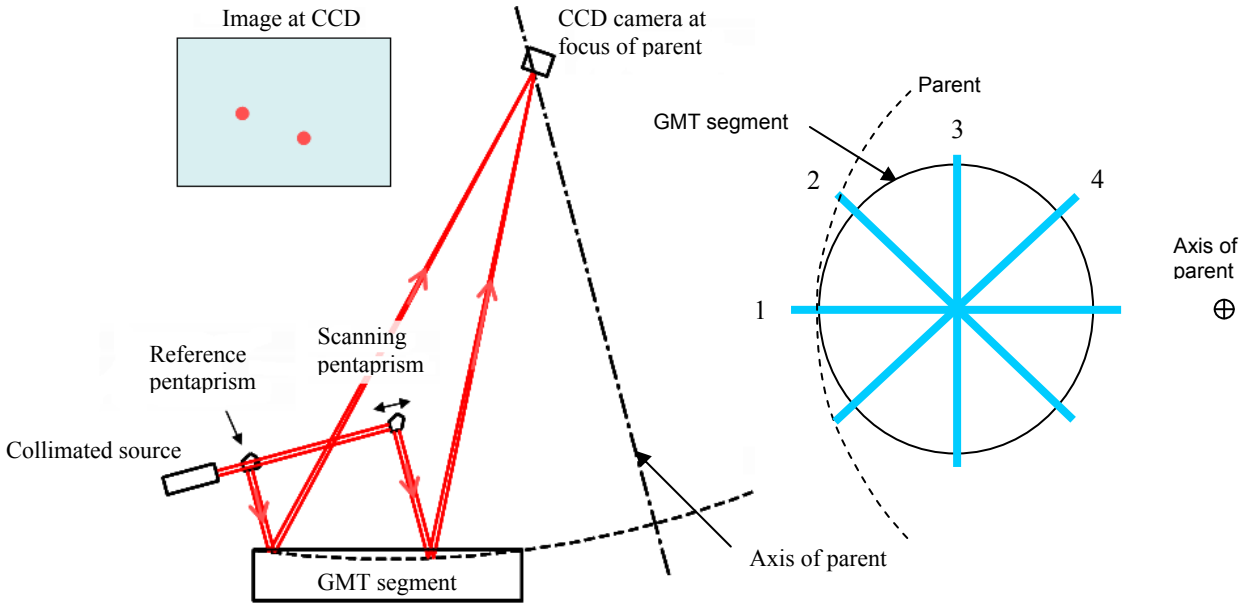

Figure 1: View of the ray paths (left) and scan paths (right) that are needed to measure low-order aberrations in the pentaprism test.

2. PRINCIPLES OF THE PENTAPRISM TEST

The collimated light source, two pentaprisms and the camera form the core of the pentaprism test system in Figure 1. The solid-body rotations of the pentaprisms with respect to the source are referred to as pitch, roll, and yaw. These parameters are defined graphically in Figure 2. The accuracy of the pentaprism system in Figure 1 relies on the fact that spot motion in one direction, referred to as the in-scan direction, is insensitive to the pitch motions of the pentaprism. Slopes on the mirror are therefore exclusively determined from spot displacements in the in-scan direction on the camera.

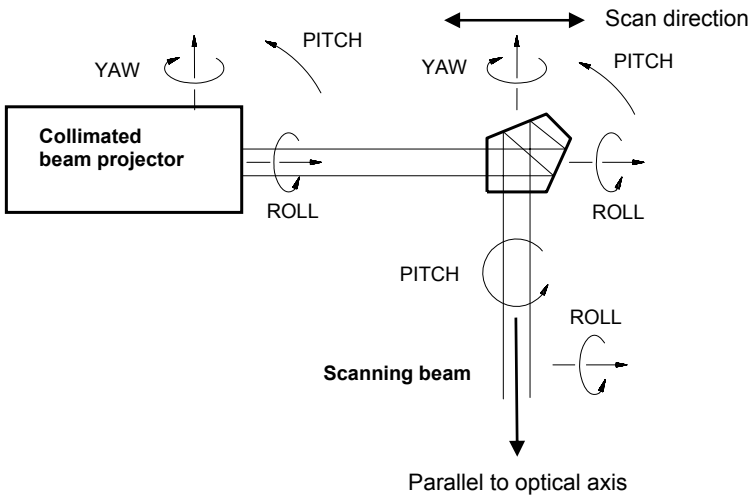

Figure 2. Defining diagram for the terms pitch, roll, and yaw.

The in-scan direction on the camera is perpendicular to the roll direction that is found by taking frames with the prisms rolled to either side of the nominal position for taking data. (A prior adjustment of prism yaw guarantees that roll and yaw produce parallel spot motion.) The reference pentaprism is placed in the system so that spot motions produced by small motions of the source and mirror can be eliminated by comparing the in-scan motions of the spots from the two prisms. If the surface under test is not parabolic, the nominal ray paths for both the scanning spot and the reference spot must be calculated before the slope error can be determined.

2.1 Effects specific to off-axis mirrors

Conceptually, the collimated beam incident on the mirror surface is parallel to the optical axis of the system. For an off-axis mirror, this is the optical axis of the parent. A change in the angle of the incoming beam is equivalent to moving to a non-zero field of view, and introduces field aberrations. The first-order effect, a tilt or constant displacement of the spot in the focal plane, is eliminated by removing the in-scan displacement of the reference spot from the in-scan displacement of the scanning spot. In addition, there are field aberrations consisting of astigmatism, coma and trefoil in fixed ratios.[7] The field aberrations represent slope errors that vary with pupil position and therefore show up in the result of the pentaprism measurement. Any change in field angle among the different scans causes variable field aberrations that cannot easily be disentangled from surface errors. A constant field angle, common to all measurements, produces a single set of field aberrations that can be separated from the fit to the mirror surface errors. A common field angle is achieved by making all scans intersect at a point near the center of the mirror, and aligning the system for each scan so the spot from this common intersection point is at the same position on the detector.

Field aberrations also complicate two features that give the pentaprism system its fundamental accuracy. These are the insensitivity of in-scan spot displacements to orientation of the pentaprisms, and the use of the reference prism to remove system misalignments including the tilt of the beam projector. Both effects are quantified in Reference [7]. In order to make use of the first feature—insensitivity to prism orientation—we must determine the in-scan direction in the focal plane to an accuracy of 0.5 mrad. This is done by rolling the pentaprism as described in Section 2. This procedure is complicated by the fact that rolling the prism is equivalent to a change in field angle and introduces field aberrations. In general, the magnitude and direction of spot displacement depend on position in the pupil. For an off-axis mirror, most scans do not pass through the optical axis and in this case the cross-scan direction changes significantly across the scan. The direction changes by 110 mrad in the worst case for the GMT segment (scan 3 in Figure 1). It is therefore necessary to repeat the roll measurement at several points along the scan, in order to determine the cross-scan direction as a function of position.

The second feature that improves the measurement accuracy—using the reference pentaprism to compensate for system misalignments—is complicated by the fact that the reference prism and scanning prism sample different points in the pupil. The ratio of the in-scan displacements depends only on the positions of the two beams in the pupil. In NST testing this ratio varied from 1 to 0.91 in the worst case (scan 1 in Figure 1).[7] In practice, in-scan displacements of the reference spot are less than 50 μrad. To reach a measurement accuracy of 0.5 μrad in wavefront slope, the ratio of displacements is calculated at least to an accuracy of 0.01, and the reference spot's displacement is scaled by this ratio before subtracting it from the scanning spot's displacement.

2.2 Measurement of a non-parabolic mirror

The GMT is an ellipsoid with k = -0.998286, and on-axis rays do not come to a common point of focus, i.e. the pentaprism test is not a null test. Figure 3 shows the distribution of camera spots that would occur if an off-axis segment were illuminated with a rectangular grid of on-axis pentaprism beams. Figure 4 isolates the spots positions that would occur in a 0° scan along path 1 in Figure 1, while Figure 5 isolates the spot positions that would occur in a 90° scan along path 3 in Figure 1. These diagrams make it clear that the expected spot positions must be accurately calculated if meaningful conclusions are to be drawn from the measurements.

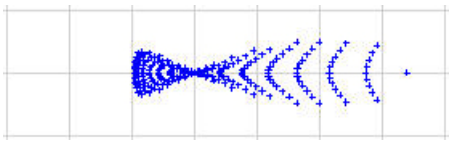

Figure 3. Spot diagram showing the camera spots that would occur if a large number of pentaprism measures were taken in a rectangular grid over the 8.4 m off-axis segment. Each division is 200 µm. The center of the camera is 17999 mm from the vertex of the parent mirror. The pattern is 874µm wide and 194 µm high. The angular distribution of the spots is 45.9 by 10.2 µrad.

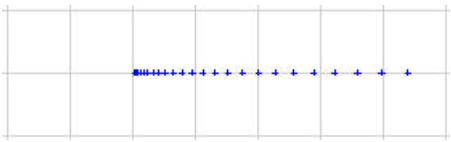

Figure 4. Spot diagram showing the camera spots that would occur in a 0 degree scan across the segment. Each division is 200 µm. The spot pattern is 874 µm across. The angular distribution of the spots is 45.9 µrad.

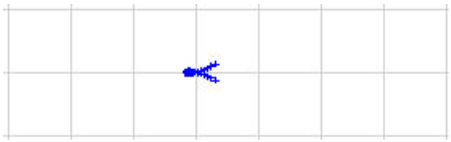

Figure 5. Spot diagram showing the camera spots that would occur in a 90 degree scan across the segment. Each division is 200 µm. The horizontal spread of the points is 96.7 µm. The vertical spread is 50.6µm. The angular spread is 5.1 µrad by 2.7 µrad.

3. MEASUREMENT OF THE NST PRIMARY MIRROR

Figure 6 shows the pentaprism system that was used to verify the 1.7 m off-axis primary mirror for the New Solar Telescope (NST). Although this mirror is a paraboloid instead of an ellipsoid, it is close to a 1/5 scale model of an off-axis GMT segment.

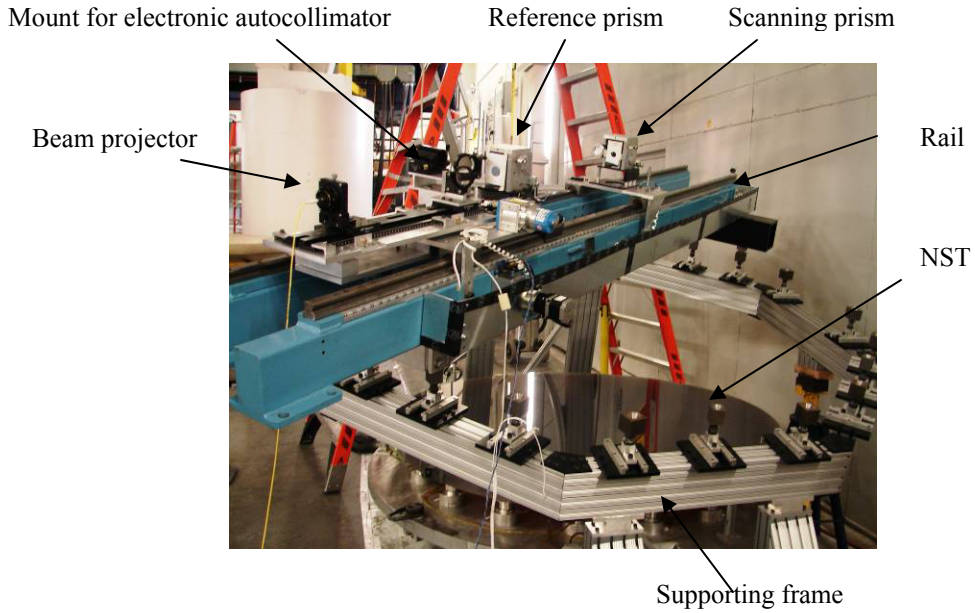

Figure 6. Pentaprism system for a test of the 1.7 m off-axis NST primary mirror.

The rail system for the source and two pentaprisms was mounted on an octagonal frame that allowed the mirror to be scanned in either direction at 4 positions separated by 45°. The pitch and roll of the rail system were manually adjusted so that the return spot from the center of the mirror fell on the same 7.4 μm camera pixel at all scan angles. Field variations at the common point were less than 1.8 μrad. Final measurements on the mirror were taken at four scan angles. Data were acquired every 20 mm across the mirror. At several points along the scan, the prism was rolled in both directions to determine the cross-scan direction to an accuracy of 0.5 mrad. Data processing consists of the following steps:

1. Use a correlation method to find the positions of the scanning and reference spots for each measurement.
2. Determine the in-scan displacements of the spots, taking account of the in-scan direction's dependence on pupil position.
3. Subtract the reference spot displacement from the scanning spot displacement, taking account of the field aberration's effect on each spot position.
4. Subtract the spot displacements due to small-scale slope errors measured in the interferometric test of the mirror.
5. Fit a model consisting of Zernike polynomials to the slope data.
6. Separate field aberrations and focus error from the surface map.

Figure 7 shows the differential in-scan spot displacements (output of step 4 above), and the best-fit model. The model is a simultaneous fit to all 4 scans. Most of the spot displacement is a focus alignment error, meaning the detector was not precisely in the best-fit focal plane. When the model is subtracted from the data, the rms residual error over all scans is 5.3 μm or 1.3 μrad rms wavefront slope.

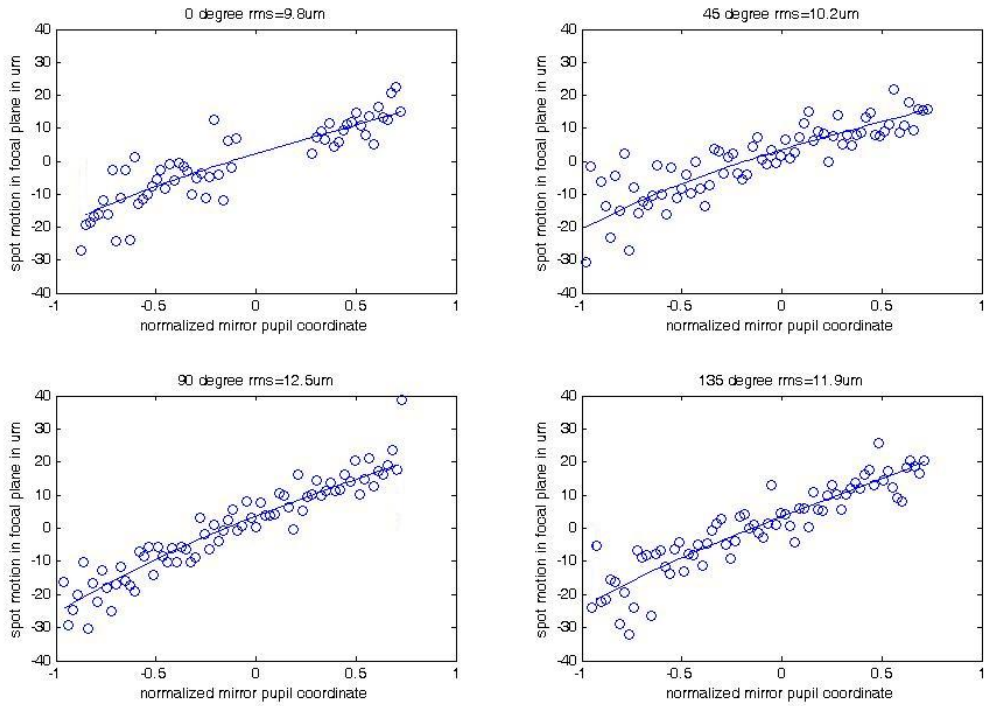

Figure 7. In-scan spot displacement vs. pupil coordinate for 4 scans of the NST mirror. The curves represent the low-order polynomial fit to the combined data set. Focus alignment error accounts for the common linear component of spot motion.

Table 1 lists the polynomial coefficients from the pentaprism measurements and compares them with a fit to the interferometric optical test. Field and focus aberrations are subtracted from both sets of polynomials. They are equivalent to departures from the nominal focal length, off-axis distance and clocking angle in the two set of measurements; these

parameters were also determined from both tests and are compared in Table 2. For the finished mirror, low-order aberrations are within the noise level of both measurements. We also measured the mirror at an early stage when low-order aberrations were significant. These results are also listed in Table 1. The measurements agree within the uncertainty of the pentaprism measurements. Figure 8 shows plots of the low-order fits at the early stage when there were significant aberrations. Similar plots for the finished mirror would show only noise.

Table 1. Polynomial fit to pentaprism and interferometer measurements of the NST mirror. Focus and field aberrations, equivalent to a fixed combination of astigmatism and coma, have been subtracted and are compared separately in Table 2. Results are listed for measurements made at two different times during the fabrication process. Uncertainties for the pentaprism measurement are determined by a Monte Carlo simulation using 1 μrad rms wavefront slope noise, 4 scans, and 37 points per scan for the early measurements and 73 points for the final measurements. The uncertainty of the interferometric test is not accurately known.

	measured at early stage in fabrication		measurements of finished mirror	
aberration	interferometer nm rms surface	pentaprism nm rms surface	interferometer nm rms surface	pentaprism nm rms surface
astigmatism 0°	8	9 ± 22	1	-1 ± 16
astigmatism 45°	0	-2 ± 22	0	0 ± 16
coma 0°	-87	-98 ± 10	1	0 ± 7
coma 90°	-4	16 ± 10	-4	8 ± 7
trefoil 0°	-50	-32 ± 30	-1	-8 ± 19
trefoil 30°	9	23 ± 30	-2	-3 ± 19
spherical	-32	-35 ± 8	-1	-4 ± 5
RSS	106	118	5	12

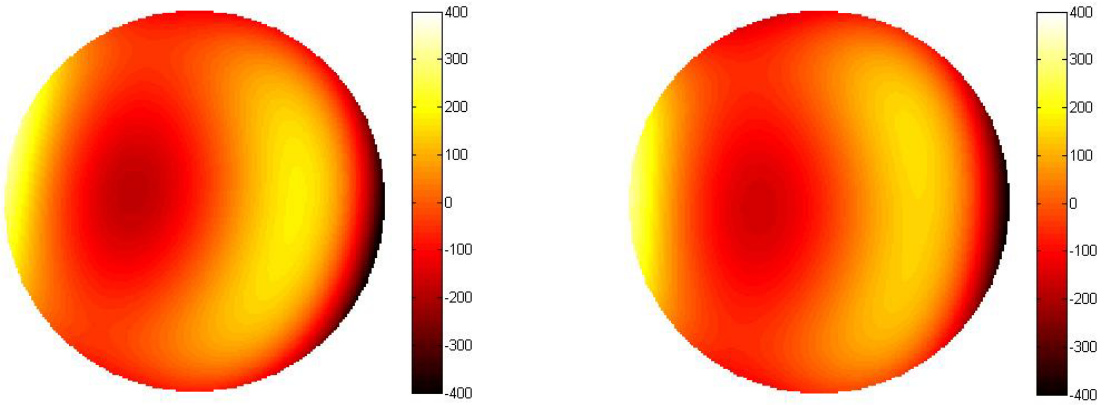

Figure 8. Low-order fit to the pentaprism test (left, with 118 nm rms surface) and the interferometric test (right, 106 nm rms) for the NST mirror at an early stage before the mirror was finished. Color bar is labeled in nm of surface error.

During the pentaprism measurements, we monitor the position of the mirror and detector with a laser tracker. This information, along with the measured focus and field aberrations, can be used to determine the mirror's focal length, off-axis distance, and clocking angle.[7] A similar analysis applies for the interferometric measurements. Table 2

compares the results of these two determinations of the mirror's geometry. The clocking angle is measured relative to fiducial scribe lines on the edge of the mirror, which are at the point directly opposite the parent axis and every 90° around. The two measurements show excellent agreement in focal length and clocking. The difference in off-axis distance is roughly at the level of measurement accuracy and well within the 5 mm tolerance.

Table 2. NST mirror geometry determined by the pentaprism test and interferometric test.

	Focal length	Off-axis distance	Clocking angle
pentaprism test	3849.9 ± 0.4 mm	1838.7 ± 1 mm	0.023°
interferometric test	3849.6 ± 0.5 mm	1840.6 ± 1 mm	0.006°

4. GMT PENTAPRISM SYSTEM

4.1 The scanning pentaprism rail

A view of the pentaprism test system and the first GMT segment is shown in Figure 9. The fiber source, collimating lens, reference pentaprism, scanning pentaprism, and associated drive hardware are all mounted on the steel box beam that is over the mirror. A large bearing connects the pentaprism rail to an arm that folds out from the side of the tower. An electrically-driven worm gear is used to rotate the rail assembly about the bearing axis. The system has a rotational range of 300°. The bearing axis and the axis of the parent mirror are both tilted 13.5° from vertical so that the mirror can be tested in a horizontal position. The parent axis is to the right of the mirror in this view.

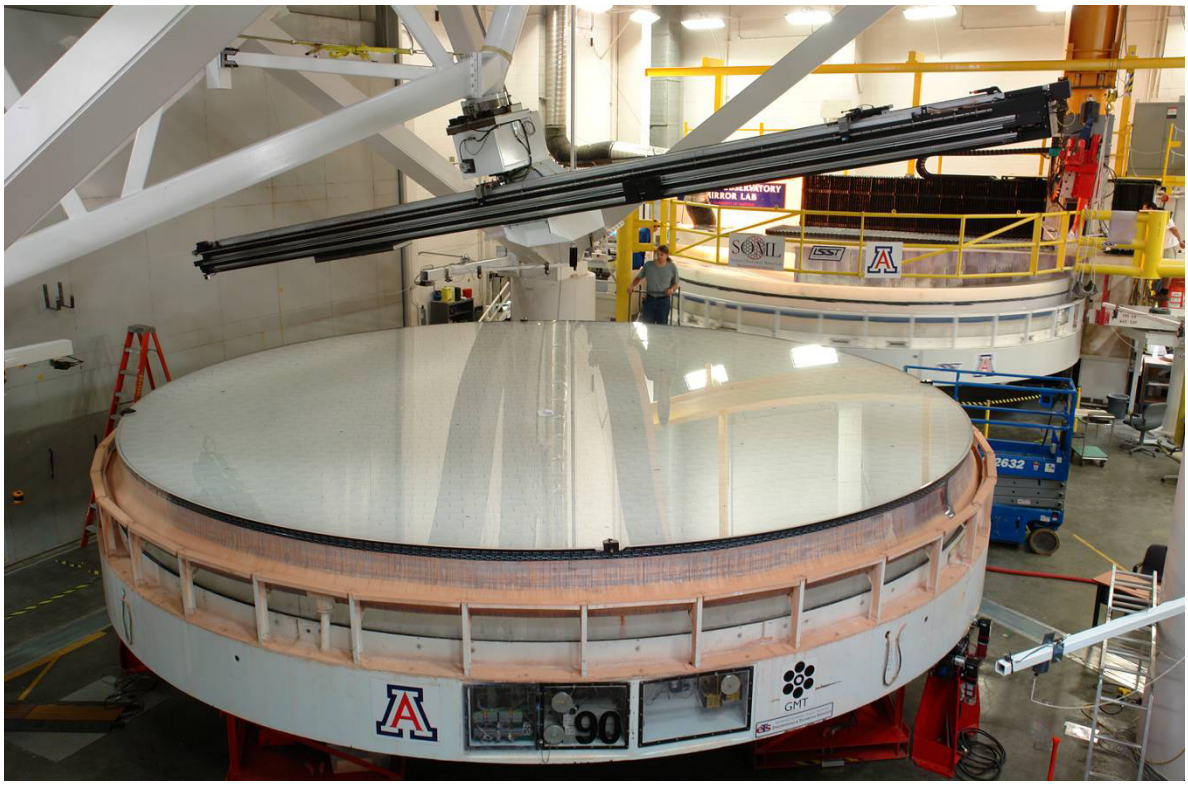

Figure 9. View of the first GMT segment in position for taking scanning pentaprism data. The tops of the pentaprism carriages are visible on the top of the box beam. The pentaprisms themselves are out of sight on the far side. The mirror for the Large Synoptic Survey Telescope is in the background. Photo by Ray Bertram, Steward Observatory.

4.2 Rail components

The source end of the pentaprism rail is shown in Figure 10. Adjustable mounts for the 635 nm fiber and the 50 mm diameter lens that produces a collimated beam for the system hang off the right side of the box beam. The mount in between them holds two UDT Instruments autocollimators that are used to monitor the yaw of the pentaprisms. The pentaprisms themselves are mounted on two carriages that ride the 1-inch diameter cylindrical rails that are on the top and left side of the box beam. Each carriage is connected to the top rail via two Thomson linear ball bearings. A single linear bearing on a flexure connects each carriage to the side rail. Scan positions have a ±2 mm uncertainty. Pitch, roll, and yaw are controlled to ±0.5 mrad by the rail system.

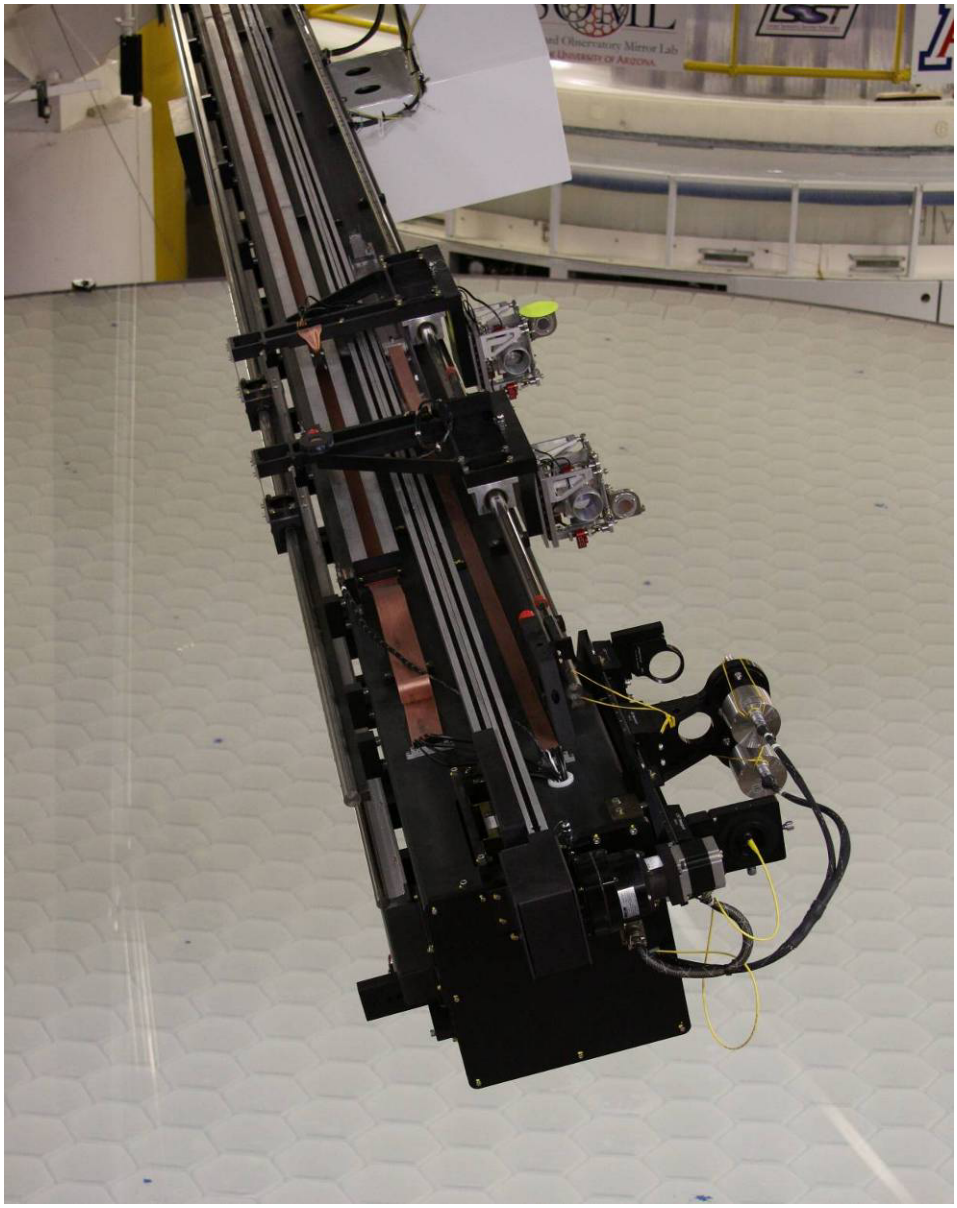

Figure 10. Top view of the source end of the GMT scanning pentaprism system. The source fiber, collimating lens, and two pentaprism carriages are on the right side of the box beam. The shiny cylinders near the source are autocollimators.

4.3 Pentaprism motions

Each pentaprism is manipulated with four picomotors in roll, yaw and translation perpendicular to the scan direction. Pitch of the prism has no first-order effect on deflection of the collimated beam, so it does not need to be controlled provided the roll and yaw are controlled to 0.5 mrad. Three of the four picomotors on the scanning carriage are visible in Figure 11. The view is from below with the carriage at the center of its travel, in line with the rail's rotational bearing axis. The mount for the autocollimator return mirror is visible on the side of the pentaprism housing. The ring on the output of the pentaprism housing is 40 mm in diameter.

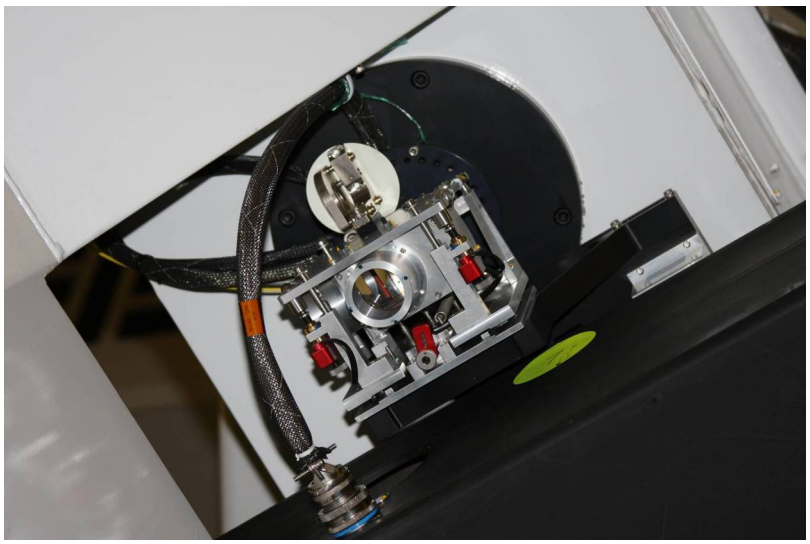

Figure 11. Bottom view of the scanning pentaprism. Each pentaprism can be manipulated with four picomotors. The red housings of three of these motors are shown here. The ring on the output of the pentaprism housing is 40 mm in diameter.

4.4 Pentaprism camera

Figure 12 shows the Apogee Instruments Alta U16000 CCD camera that was selected for use in the pentaprism test. The Kodak KAI-16000M chip in this camera has an active area of 36 x 24 mm, and the pixels are 7.4 x 7.4 microns in size. The figure shows a point source microscope being used to determine the position of the camera chip with respect to four tracker balls on its mounting plate.

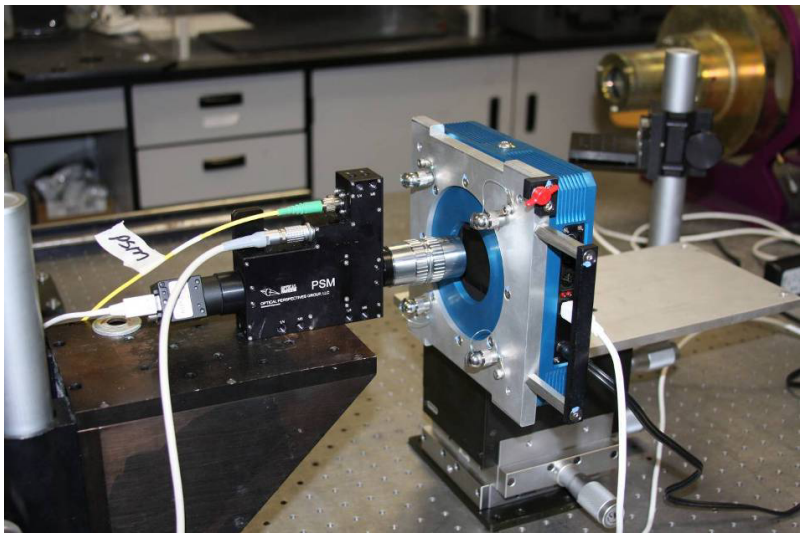

Figure 12. The Alta U-16000M camera used in the pentaprism test. The point source microscope on the left is being used to measure the position of the camera chip with respect to the four tracker balls on its mount. The laser tracker itself is out of view to the left.

4.5 Preliminary data set

A preliminary set of GMT pentaprism data was taken June 2, 2010. The measurements provide a baseline data set which can be used to make improvements in the hardware, the data taking software, and the downstream processing. A graph of the pentaprism data from a scan at 225° is shown in Figure 13. The entire 36 x 24 mm field of the camera is displayed on the graph. The scanning prism data form the large cluster of spots just below center. The reference data are just above it to the right. The 4 widely-separated spots were taken with the prisms rolled to either side of the nominal position. The in-scan direction for each prism is defined to be perpendicular to the line between the roll spots.

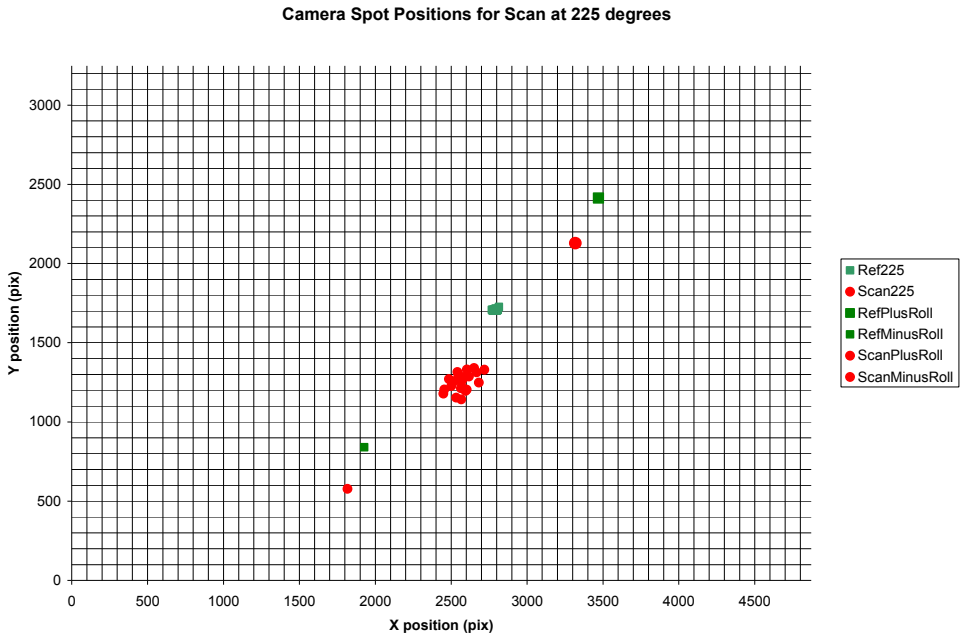

Figure 13. Plot of the spot positions that were measured during the first scan at 225°. Spots from the scanning prism are clustered just below center. Spots from the reference prism are up and slightly to the right of center. Four spots taken during the roll angle calibration are also shown. The full area of the camera chip is displayed.

5. PENTAPRISM PERFORMANCE

5.1 Performance requirements

The most important function of the pentaprism test is to verify the accuracy of low-order aberrations measured in the interferometric optical test (the principal test). Alignment of the principal test is challenging, and any mistake in alignment would cause low-order aberrations, in particular focus, astigmatism, coma and trefoil. The accuracy requirement for these aberrations is based on the use of active optics at the telescope: the wavefront will be measured and low-order aberrations (including manufacturing errors) will be corrected by adjusting the alignments of the segments and by bending the segments with their 165-actuator active support systems. For correction of manufacturing errors, these adjustments are limited to no more than 2 mm displacement of the segment from its nominal alignment, and no more than 42 N rms support force to bend out the remaining errors. The accuracy requirement for low-order aberrations is therefore that they must be correctable within these limits. No specific limits are placed on individual aberrations. Our goal is to limit the error in each aberration to a magnitude that can be corrected with 10 N rms support force. Errors on smaller spatial scales—those not treated as low-order aberrations—must satisfy a separate specification for figure error as a function of spatial scale.

Accuracy requirements for radius of curvature, off-axis distance and clocking angle are based on the same principles. An error in radius of curvature is considered a focus error and treated like the other low-order aberrations. Errors in off-axis distance and clocking can be corrected by adjusting the segment's alignment in the telescope, so they

must be determined to an accuracy within the 2 mm limit on displacement. These parameters are determined by combining the pentaprism measurements of the wavefront with laser tracker measurements of the position of the mirror and the detector.

5.2 Slope measurement at a single point

Table 3 shows the high-level error budget for individual slope measurements in the GMT pentaprism test. The different terms in the error budget are explained below. The values listed are estimates and are thought to be conservative.

Table 3. High-level error budget for measurement of wavefront slope at a single scan position. The net error is 1 μrad rms.

Source of error	rms wavefront slope (nrad)
determination of spot positions	600
aliasing of mirror figure error	400
optical alignment	500
thermal effects	400
margin	260
sum in quadrature	1000

The error budget in Table 3 requires that we determine the position of each of the two spots to about 0.42 μrad. Diffraction causes the camera spots to be 16 μrad in diameter. In terms of angle, the spot size and accuracy requirement are the same as for the NST measurement. We use a correlation technique (comparing the measured intensity distribution to a pre-recorded distribution, and finding the maximum correlation) that is capable of determining spot positions to the required accuracy.

The pentaprism measurements will be taken at intervals between 200 and 400 mm across the mirror. Because the measurements will be widely spaced, small-scale figure errors will be aliased into the low-order aberrations we want to measure. For this reason, the pentaprism test is most accurate for measuring a nearly completed segment. We will subtract from the pentaprism data the small-scale slope errors determined by the high-resolution interferometric measurement.

System alignment errors are all second-order effects, including coupled errors in pitch, roll and yaw. We have set each alignment parameter to an accuracy of 0.5 mrad, and we allow up to 0.2 mrad rms variations across a scan. The picomotors are used to make adjustments in roll and yaw. Each prism has its own autocollimator for monitoring yaw, and roll is controlled based on the cross-scan displacement of the spot.

The pentaprisms are made of BK7 and are somewhat sensitive to temperature gradients in the glass. Only the variations in temperature gradient during a 10-15 minute scan contribute errors to the measured aberrations. The error budget allows variations of about 0.2 K/m, or about 0.01 K through the prism, during the course of the scan.

5.3 Determination of low-order aberrations and mirror geometry

The accuracy with which the low-order aberrations can be measured depends on the accuracy of the slope measurements, the number of sample points per scan, the number of scans, and the extent to which errors are correlated among sample points and scans. We have determined the measurement accuracy for each aberration by simulating a measurement set of 4 scans, every 45°, and uncorrelated noise of 1 μrad rms wavefront slope per point. For sampling of 20 points per scan, we expect to have the errors listed in Table 4. The mirror specifications on radius of curvature, off-axis distance, and clocking angle are also compared to estimates of the accuracy that can be achieved in the pentaprism test, including laser tracker measurements of the test geometry. The goals listed for low-order aberrations represent the amounts that can be corrected with the active support system using 10 N rms forces for each aberration.

The pentaprism system will meet all its requirements and goals comfortably, with the possible exception of radius of curvature. The net uncertainty for this parameter—a combination of focus in the wavefront measurement and distance between mirror and detector—is expected to be 0.4 mm. The principal test has similar accuracy in radius of curvature while the Laser Tracker Plus measurement is expected to give an accuracy of 0.3 mm. A radius error of 0.4 mm would be corrected at the telescope by shifting the segment alignment by 0.9 mm along a line through the parent axis, an acceptable motion.

Table 4. Mirror specifications and goals, and expected accuracy of the pentaprism system, for the GMT segment. Goals listed for low-order aberrations are rms surface error in each component. Expected pentaprism accuracy for these aberrations is based on the simulation described in the text. Expected accuracy for mirror geometry is based on the wavefront measurement combined with laser tracker measurements of the test geometry.

parameter	specification	goal	pentaprism accuracy
radius of curvature	±0.5 mm	±0.3 mm	±0.4 mm
off-axis distance	±2.0 mm	±1.0 mm	±0.2 mm
clocking angle	±50 arcsec		±5 arcsec
astigmatism		830 nm	120 nm
coma		71 nm	42 nm
trefoil		180 nm	85 nm

6. SUMMARY

The GMT scanning pentaprism system will provide an independent measurement of the low-order aberrations in the off-axis segments. The test methodology has been thoroughly analyzed, including a number of important effects that are specific to off-axis mirrors. A prototype of the GMT system was used to measure the 1.7 m off-axis NST mirror. This system was found to be sensitive to 1 μrad rms wavefront errors and produced results in excellent agreement with an interferometric optical test. The GMT pentaprism system promises to have a performance similar to the NST system and should therefore meet all the requirements for testing the 8.4 m off-axis segments.

REFERENCES

[1] M. Johns, "Progress on the GMT", *Ground-based and Airborne Telescopes II*, Proc. SPIE 7012, 70121B (2008).

[2] M. Johns, "The Giant Magellan Telescope (GMT)", *Ground-based and Airborne Telescopes*, Proc. SPIE 6267, 626729 (2006).

[3] H. M. Martin, R. G. Allen, J. H. Burge, D. W. Kim, J. S. Kingsley, M. T. Tuell, S. C. West, C. Zhao and T. Zobrist, "Fabrication and testing of the first 8.4 m off-axis segment for the Giant Magellan Telescope", *Modern Technologies in Space- and Ground-based Telescopes and Instrumentation*, Proc. SPIE 7739 (2010).

[4] James H. Burge, *Advanced Techniques for Measuring Primary Mirrors for Astronomical Telescopes*, Ph.D. Dissertation, Optical Sciences, University of Arizona (1993).

[5] J. H. Burge, L. B. Kot, H. M. Martin, C. Zhao and T. Zobrist, "Alternate surface measurements for GMT primary mirror segments", *Optomechanical Technologies for Astronomy*, Proc. SPIE 6273, 62732T (2006).

[6] Peng Su, James H. Burge, Brian Cuerden, Jose Sasian, Hubert M. Martin, "Scanning pentaprism measurements of off-axis aspherics," Proc. SPIE 7018, 70183T (2008).

[7] Peng Su, James H. Burge, Brian Cuerden, Richard Allen, Hubert M. Martin, "Scanning pentaprism measurements of off-axis aspherics II," Proc. SPIE 7426, 74260Y (2009).